

# *In vitro* and *in vivo* human metabolism of the synthetic cannabinoid AB-CHMINACA

Claudio Erratico,<sup>†</sup> Noelia Negreira,<sup>†</sup> Helia Norouzizadeh, Adrian Covaci, Hugo Neels, Kristof Maudens and Alexander L.N. van Nuijs\*



N-[(1S)-1-(aminocarbonyl)-2-methylpropyl]-1-(cyclohexylmethyl)-1H-indazole-3-carboxamide (AB-CHMINACA) is a recently introduced synthetic cannabinoid. At present, no information is available about *in vitro* or *in vivo* human metabolism of AB-CHMINACA. Therefore, biomonitoring studies to screen AB-CHMINACA consumption lack any information about the potential biomarkers (e.g. metabolites) to target. To bridge this gap, we investigated the *in vitro* metabolism of AB-CHMINACA using human liver microsomes (HLMs). Formation of AB-CHMINACA metabolites was monitored using liquid chromatography coupled to time-of-flight mass spectrometry. Twenty-six metabolites of AB-CHMINACA were detected including seven mono-hydroxylated and six di-hydroxylated metabolites and a metabolite resulting from *N*-dealkylation of AB-CHMINACA, all produced by cytochrome P450 (CYP) enzymes. Two carboxylated metabolites, likely produced by amidase enzymes, and five glucuronidated metabolites were also formed. Five mono-hydroxylated and one carboxylated metabolite were likely the major metabolites detected. The involvement of individual CYPs in the formation of AB-CHMINACA metabolites was tested using a panel of seven human recombinant CYPs (rCYPs). All the hydroxylated AB-CHMINACA metabolites produced by HLMs were also produced by the rCYPs tested, among which rCYP3A4 was the most active enzyme. Most of the *in vitro* metabolites of AB-CHMINACA were also present in urine obtained from an AB-CHMINACA user, therefore showing the reliability of the results obtained using the *in vitro* metabolism experiments conducted to predict AB-CHMINACA *in vivo* metabolism. The AB-CHMINACA metabolites to target in biomonitoring studies using urine samples are now reliably identified and can be used for routine analysis. Copyright © 2015 John Wiley & Sons, Ltd.

Additional supporting information may be found in the online version of this article at the publisher's web site.

**Keywords:** AB-CHMINACA; *in vitro* metabolism; human liver microsomes; LC-QTOF/MS

## Introduction

In recent years, an increasing number of new psychoactive substances (NPS) have been released on the drug market. In 2012, the United Nations Office on Drugs and Crime estimated that more than 340 different NPS were available worldwide.<sup>[1]</sup> These substances mimic the effects of regulated drugs of abuse such as cocaine, ecstasy, and cannabis but they are often not controlled by law. Therefore, surveillance programs monitoring the use of law regulated drugs in the general population likely miss the use of the newly released NPS. Also, NPS are marketed without any pharmacokinetic, clinical or toxicological information and, as a consequence, users of these drugs can suffer from severe (and sometimes lethal) side effects.

The largest class of NPS is probably the group of the synthetic cannabinoids with 105 individual substances currently monitored in the European Union.<sup>[2]</sup> Many synthetic cannabinoids (and some of their metabolites) are full or partial agonists of the cannabinoid type 1 or type 2 receptors.<sup>[3–6]</sup> Therefore, these synthetic compounds can exert psychotropic and sedative effects similar to those of the natural psychoactive cannabinoid  $\Delta^9$ -tetrahydrocannabinol.<sup>[7,8]</sup> Adverse effects associated with the use of synthetic cannabinoids include acute psychosis, anxiety, hypertension, agitation, and seizures.<sup>[8]</sup> However, profound knowledge about the toxic effects of synthetic cannabinoids in particular is still very limited and, therefore, requires further research.<sup>[8]</sup>

Several families of synthetic cannabinoids can be identified according to their chemical structure.<sup>[2]</sup> Drugs belonging to the

AB-INACA family, which appeared on the market only very recently, share an indazole-carboxamide (INACA) backbone with an extra amino-methyl-oxobutanyl (AB) group (Figure 1).<sup>[9]</sup> To the authors knowledge, currently the AB-INACA family includes N-(1-amino-3-methyl-1-oxobutan-2-yl)-1-(4-fluorobenzyl)-1H-indazole-3-carboxamide (AB-FUBINACA), N-(1-amino-3-methyl-1-oxobutan-2-yl)-1-pentyl-1H-indazole-3-carboxamide (AB-PINACA), 5-fluoro-AB-PINACA, 5-chloro-AB-PINACA<sup>[10]</sup> and N-[(1S)-1-(aminocarbonyl)-2-methylpropyl]-1-(cyclohexylmethyl)-1H-indazole-3-carboxamide (AB-CHMINACA). AB-PINACA and AB-FUBINACA have been identified in products sold online in Japan in 2013<sup>[11]</sup> and AB-CHMINACA was detected in postmortem specimens from a multiple drug intoxication in Japan in 2014,<sup>[12]</sup> suggesting that the use of drugs belonging to the AB-INACA family is becoming more wide spread. The Drug Enforcement Administration of the United States of America reports adverse effects such as seizures, coma, severe agitation, loss of motor control, loss of consciousness, difficulty breathing, altered mental status, and convulsions that in some cases resulted in death related with the use of AB-CHMINACA and AB-PINACA.<sup>[13]</sup>

\* Correspondence to: Dr Alexander van Nuijs: Toxicological Center, Universiteit Antwerpen, Universiteitsplein 1, 2610, Wilrijk-Antwerpen, Belgium. E-mail: alexander.vannuijs@uantwerpen.be

<sup>†</sup> co-first author/ these two authors contributed equally to the present study.

Toxicological Center, Department of Pharmaceutical Sciences, University of Antwerp, Universiteitsplein 1, 2610 Wilrijk-Antwerp, Belgium

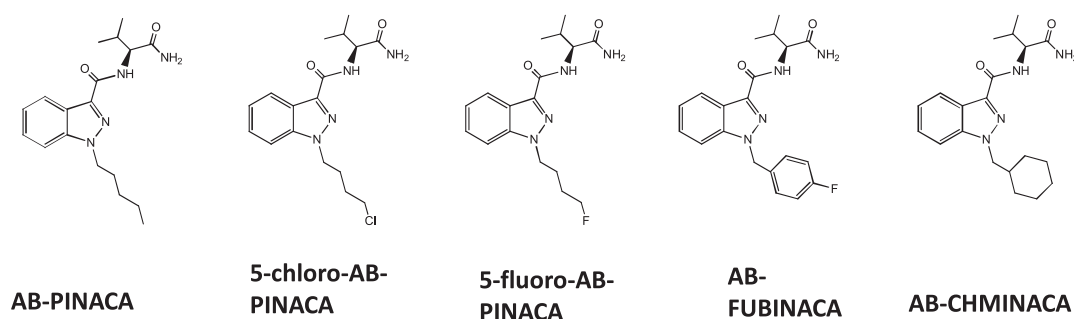


**Figure 1.** Structure of the drugs belonging to the AB-INACA family.

Very limited information about human metabolism of the drugs belonging to the “AB-INACA” family is presently available. In particular, only two studies investigating the Phase I metabolism of AB-PINACA and AB-FUBINACA by human liver microsomes (HLMs) have been published.<sup>[14,15]</sup> In these studies, formation of carboxylated and hydroxylated metabolites of AB-PINACA and AB-FUBINACA were observed. However, Phase II metabolism of these two compounds was not investigated. Also, to the authors’ knowledge, no information about AB-CHMINACA metabolism is currently available.

Information about the drug metabolism in humans is of high importance. Typically drugs show a medium degree of lipophilicity.<sup>[16]</sup> Therefore, it is likely that they are poorly soluble in polar media, like urine, where they can be present in low concentrations, which make their detection an analytical challenge, therefore increasing the possibilities of false-negative results. In contrast, usually drug metabolism results in the formation of metabolites which are more hydrophilic than the parent compound and, therefore, are more soluble in urine and are excreted from the body more readily than their parent compound. As a consequence, metabolites can be present at higher concentrations than their parent compound in urine. Therefore, knowledge about the structure of the drug metabolites formed in humans substantially improves the ability to monitor the use of drugs through a selection of the best available metabolic biomarkers.

The aims of the present study were (1) to elucidate the *in vitro* metabolic pathway of the synthetic cannabinoid AB-CHMINACA using human liver microsomes; (2) to identify the individual enzymes responsible for the formation of the metabolites; (3) to determine the human *in vivo* AB-CHMINACA metabolites excreted in the urine obtained from an AB-CHMINACA user; and (4) to compare the human *in vitro* and *in vivo* metabolites of AB-CHMINACA detected to identify the most reliable AB-CHMINACA metabolites to use in biomonitoring studies.

## Materials and methods

### Chemicals and reagents

The standard for AB-CHMINACA was obtained from Cayman Chemical Company (Ann Arbor, MI, USA) in neat powder. The standards for theophylline, benzamide, tramadol, 4-nitrophenol, 2,6-uridine-diphosphate glucuronic acid (UDPGA), alamethicin and NADPH (all neat, purity >99%) were obtained from Sigma-Aldrich (Diegem, Belgium). Pooled human liver microsomes (HLMs; mix gender, n=200) were purchased from Tebu-bio (Boechout, Belgium). Baculovirus-insect cell microsomes containing expressed human CYP enzyme (CYP1A2, 2B6, 2C9, 2C19, 2D6, 2E1 or 3A4) co-expressed with human CYP oxidoreductase and human

cytochrome b5 were purchased from BD Biosciences (Erembodegem, Belgium) and Tebu-Bio. Ultrapure water was prepared using a Purelab flex water system from Elga (Tienen, Belgium). Methanol, acetonitrile and formic acid were purchased from Merck (Darmstadt, Germany). All organic solvents were HPLC grade or higher.

### *In vitro* metabolism assays

*In vitro* metabolism of AB-CHMINACA was investigated using a two-tiered approach. Tier I experiments investigated the formation of the primary Phase I (Tier IA) and secondary Phase II (Tier IB) metabolites of AB-CHMINACA. Tier II experiments investigated the formation of the major metabolites of AB-CHMINACA over a range of incubation times, protein concentrations and substrate concentrations to show that (1) the same metabolites are consistently formed over a range of different incubation conditions; (2) the amount of each metabolite formed depends on incubation time, protein concentration and substrate concentration (as it should be for a metabolite); and (3) to rank the metabolites as major, intermediate and minor *in vitro* and predict their *in vivo* ranking.

In Tier IA, samples investigating CYP-mediated metabolism of AB-CHMINACA were prepared mixing 100 mM potassium phosphate buffer (pH 7.4), HLMs (0.5 mg/mL, final concentration) and AB-CHMINACA (10  $\mu$ M, final concentration) on ice (final volume: 990  $\mu$ L). The total concentration of methanol was 1% of the final reaction mixture volume. After 5-min pre-incubation in a shaking water bath at 37 °C, the reaction was initiated by addition of 10  $\mu$ L of NADPH solution (1 mM, final concentration). An extra aliquot of NADPH was added every hour to keep its concentration saturating. The reaction was stopped after 3 h by adding 250  $\mu$ L of an ice-cold acetonitrile solution containing 1% formic acid v/v and 5.0  $\mu$ g/mL of theophylline (used as internal standard because it can be ionized in either ionization polarity). The samples were vortexed for 30 s and centrifuged at 8,000 rpm for 5 min. The supernatant was transferred to a glass tube, evaporated to dryness under a nitrogen gas stream at 60 °C and resuspended in 200  $\mu$ L of ultrapure water before transferring it to a vial for analysis.

Samples investigating the amidase-mediated metabolism of AB-CHMINACA were prepared as described above omitting NADPH. Because amidases do not need a cofactor, the reaction was initiated by addition of HLMs, which were pre-incubated for 5 min at 37 °C alongside the metabolism samples. Samples investigating 2,6-uridinediphosphate glucuronosyl transferases (UGTs) mediated metabolism of AB-CHMINACA were prepared as described above for CYP enzyme samples, but adding a 10  $\mu$ L aliquot of alamethicin (10  $\mu$ g/mL, final concentration) dissolved in dimethyl sulfoxide before pre-incubating the samples. The cofactor was UDPGA instead of NADPH (1 mM, final concentration). An aliquot of UDPGA was

added to the reaction mixture every hour, consistently to NADPH in the CYP experiments.

In Tier IB, formation of glucuronidated (Phase II) metabolites of the Phase I metabolites produced in the Tier IA experiments was investigated. Phase I metabolites of AB-CHMINACA were produced as described in Tier IA. The reaction was quenched by keeping the samples on ice for 5 min, followed by centrifugation at 8000 rpm for 5 min. Then, 940  $\mu\text{L}$  of the supernatant, containing the fraction of non-metabolized drug and its metabolites generated by CYP and/or amidase enzymes, was transferred to a new tube containing a fresh aliquot of pooled HLMs (0.5 mg/mL, final concentration). Alamethicin and UDPGA were added at the concentrations and time intervals described above for Tier IA samples. The incubation time was 3 h and samples were processed as described above.

In Tier II, formation of AB-CHMINACA metabolites produced by CYP and amidase enzymes was monitored over a range of incubation times (10–90 min), protein concentrations (0.2–0.8 mg/mL) and substrate concentrations (1–10  $\mu\text{M}$ ). Samples were prepared and processed as described above in Tier IA.

Positive and negative control samples for each family of enzymes of interest were prepared as described above. For CYPs and UGTs, three different negative control samples were prepared omitting the enzymes (HLMs), the substrate (AB-CHMINACA) or the cofactor (NADPH or UDPGA) in the reaction mixture. For amidases, only substrate and enzyme negative control samples were prepared. Positive control samples were prepared using tramadol, benzamide and 4-nitrophenol as marker substrates for CYPs, amidases and UGTs, respectively.<sup>[17,18]</sup> Formation of *N*- and *O*-dealkylated tramadol metabolites, benzoic acid and the 4-glucuronidated nitrophenol was monitored.

The role of individual human CYP enzymes in the formation of AB-CHMINACA metabolites was investigated using a panel of seven human recombinant CYPs (rCYPs): rCYP1A2, 2B6, 2C9, 2C19, 2D6, 2E1 and 3A4. Reaction mixtures were prepared as described above for the Tier IA experiment, but using one human rCYP (20 pmol/mL, final concentration) per sample instead of HLMs. The reaction was allowed to proceed for 60 min. Enzyme negative control samples were prepared omitting the human rCYP. Samples were processed as described above.

### Investigation of AB-CHMINACA metabolites in a human urine sample

A urine sample from an AB-CHMINACA user was collected (approximately 7 h after the intake of the substance) by the medical staff at hospital admission due to adverse effects. A 50  $\mu\text{L}$  aliquot of urine obtained from an AB-CHMINACA user was diluted with 150  $\mu\text{L}$  of acetonitrile and vortexed for 30 s. The sample was then spun at 10,000 rpm for 2 min. The supernatant was then transferred into an HPLC vial for analysis.

### Analytical methods

The liquid chromatography-quadrupole-time-of-flight mass spectrometry (LC-QTOF-MS) system used consisted of a 1290 Infinity LC (Agilent Technologies, Santa Clara, CA, USA) coupled to a 6530 Accurate-Mass QTOF-MS (Agilent Technologies, Santa Clara, CA, USA). The instrument was operated in the 2 GHz (extended dynamic range) mode, which provides an FWHM resolution of ca. 4700 at  $m/z$  118 and ca. 10,000 at  $m/z$  922. Chromatographic separation of the AB-CHMINACA metabolites formed *in vitro* and present in human urine was achieved using a C<sub>8</sub> Zorbax Eclipse Plus column (150  $\times$  2.1 mm, 3.5  $\mu\text{m}$ , Agilent Technologies, Santa Clara,

CA, USA). The mobile phase consisted of (A) 0.1% formic acid in water and (B) 0.1% formic acid in acetonitrile. The column was kept at 30 °C and the gradient program was as follows: 10% B from 0 to 2 min, then linearly increased to 35% B from 2 to 10 min and from 35% to 85% B from 10 to 35 min followed by 85% B isocratic elution from 35 to 36 min. At 36.1 min, B was decreased to 10% until 43 min for column equilibration. The flow rate and the injection volume were set at 0.18 mL/min and 5  $\mu\text{L}$ , respectively. Formation of benzoic acid (amidase positive control) was analyzed using the same apparatus and LC column mentioned above. The mobile phases consisted of (A) water and (B) methanol. The gradient program was as follows: 50% B for the first 2 min followed by linear increase of B from 50 to 80% from 2 to 8 min. At 8.1 min, B was decreased to 50% and kept at 50% until 15 min. The flow and the injection volume were 0.2 mL/min and 5  $\mu\text{L}$ , respectively.

The QTOF-MS was tuned and calibrated (mass accuracy within  $\pm 2$  ppm) before each analysis using a solution containing reference masses (Agilent Technologies, Santa Clara, CA, USA) up to 1700 mass-to-charge ratio ( $m/z$ ). Samples were analyzed using positive and negative electrospray ionization modes (+/-ve ESI), with gas temperature at 300 °C; gas flow at 8 L/min; nebulizer pressure at 40 psi; sheath gas temperature at 325 °C; sheath gas flow at 11 L/min. Capillary and fragmentor voltages were set to 3500 and 90 V, respectively. The QTOF-MS was set to acquire  $m/z$  ranging between 50 and 1000 amu at a scan rate of 2.5 spectra per s (400 ms/spectrum). The auto-MS/MS feature was used to obtain MS/MS spectra of precursor ions, using three different collision energy values (10, 20, and 40 eV). During analysis, the mass accuracy of the QTOF was constantly monitored by measuring the reference masses with  $m/z$  values of 121.0508 and 922.0097 for positive ESI mode and of 112.9856 and 966.0007 for negative ESI mode.

### Data analysis

Data were analyzed using a two-strategy approach. First, structures of candidate metabolites of AB-CHMINACA were predicted using Nexus software (v1.5, Lhasa Limited). Starting from the chemical structure of the substrate and selecting the species of interest (i.e., humans) and the families of enzymes that might be involved in AB-CHMINACA metabolism, the software produces a list of candidate metabolites and their structures. This list was updated with the structures of additional candidate metabolites predicted by the authors. The second strategy is based on manual sieving using the Mass Hunter Workstation software (Agilent Technologies, Santa Clara, CA, USA). To identify peaks representing AB-CHMINACA metabolites and to elucidate the structure of each metabolite the following criteria were applied: (1) the measured molecular  $m/z$  of the precursor ion should be within 10 ppm of its theoretical value; (2) the measured  $m/z$  of the product ions should be within 25 ppm of its theoretical value; (3) the proposed chemical structure of the detected metabolite has to be explainable considering the chemical structure of the substrate and the reactions that the family of enzymes present in the sample analyzed is able to catalyze; (4) the absence of the candidate metabolite at the same retention time in all the negative control samples; (5) the retention time of the detected metabolites should not be higher than that of the parent drug (exceptions to be clearly explained on the basis of the proposed metabolite structure); and (6) the amount of metabolite formed had to show an increasing trend over the incubation time, protein concentration and substrate concentration ranges assessed.

Tier II data are presented as response values (calculated as the ratio of the metabolite and the internal standard peak area) to

compensate for the inter-sample variability in the analysis. The retention time and precursor ion values as well as MS/MS spectra obtained for the AB-CHMINACA *in vitro* metabolites were used to identify its metabolites present in the urine sample analyzed.

## Results

### AB-CHMINACA metabolites produced by amidase enzymes

The MS/MS spectrum of AB-CHMINACA was first investigated (Figure 2). The ion value measured at  $m/z$  357.2284 represents the protonated precursor ion of AB-CHMINACA (mass error of 1.96 ppm; Table S1). Four major product ions at  $m/z$  340.2031, 312.2087, 241.1352 and 145.0401 were observed. The first two product ions resulted from the loss of the terminal amine and amide group, respectively (mass error 3.23 and 5.45 ppm, respectively). The last two product ions are the indazole-3-carbaldehyde moiety, with and without the methyl-cyclohexyl group (mass error 6.64 and 3.45 ppm, respectively).

Two carboxylated metabolites, M20 and M21 (mass error of the precursor ions 1.54 and 2.51 ppm, respectively; Table S1) were detected when AB-CHMINACA was incubated with HLMs (with or without NADPH). These metabolites were not detected in the negative control samples for AB-CHMINACA or HLMs. M20 and M21 eluted earlier (26.7 min) and later (31.3 min) than AB-CHMINACA (28.4 min), suggesting that M20 and M21 are slightly more and less polar than AB-CHMINACA, respectively. Furthermore, the amount of M20 and M21 formed showed an increasing trend with increasing incubation times, protein concentrations and substrate concentrations. M21 was consistently formed in an amount 10 to 20 folds higher than M20 in all the samples (Figure 3). These results suggest that M20 and M21 are metabolites of AB-CHMINACA produced by HLM enzymes that do not need NADPH and, therefore, are not CYPs. The structure of M20 and M21 was further investigated using their MS/MS spectra, which contained  $m/z$  145.0435, 241.1409 and  $m/z$  145.0396, 241.1342 and 312.2075, respectively (Figure 4). These fragmentation patterns suggest a large overlap of the chemical structures of AB-CHMINACA, M20 and M21. The slight difference in fragmentation pattern of M21 and AB-CHMINACA is the presence of the ion with  $m/z$  312 (exact mass  $m/z$  312.2075), which suggests that the propyl group is still part of the molecule (Figure 4A). The structure of product ions with  $m/z$  241.1342 and 145.0396 are the indazole-3-carbaldehyde moiety with and without the methyl-cyclohexyl group (mass error 2.49 and 0 ppm, respectively). The precursor mass of M20 ( $m/z$  259.1526) together with its observed fragmentation pattern suggest that the outer amide group of AB-CHMINACA is not present in M20 (Figure 4B). Therefore, M20 and M21 result from the hydrolysis of the inner and outer amide group, respectively, forming the corresponding carboxylic acids. Because

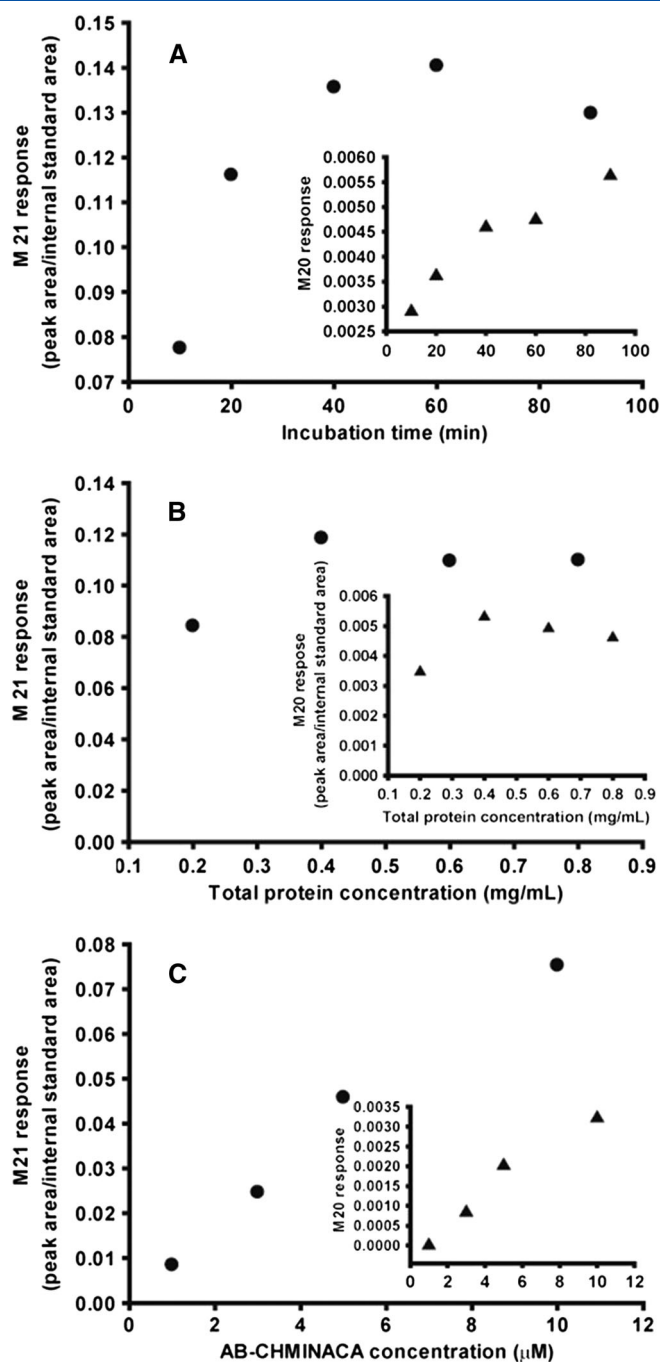


**Figure 3.** Amount of carboxylated metabolites of AB-CHMINACA (M20 and M21) formed as a function of (A) incubation time, (B) protein concentration and (C) AB-CHMINACA concentration.

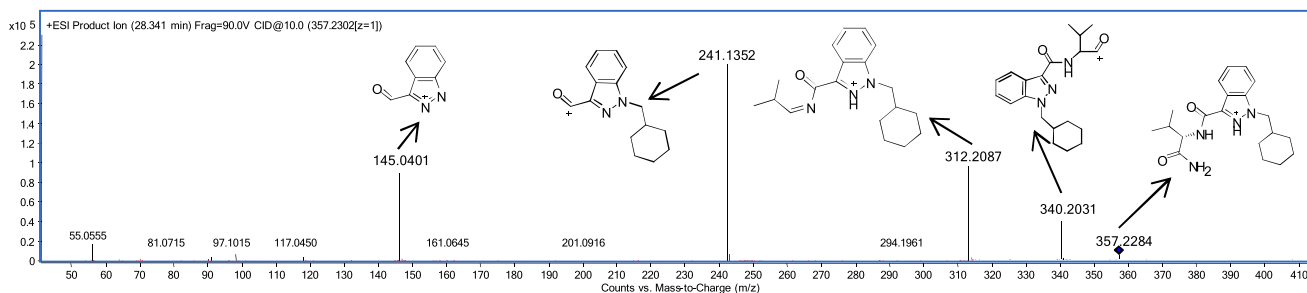


**Figure 2.** Fragmentation (MS/MS) spectrum of AB-CHMINACA.

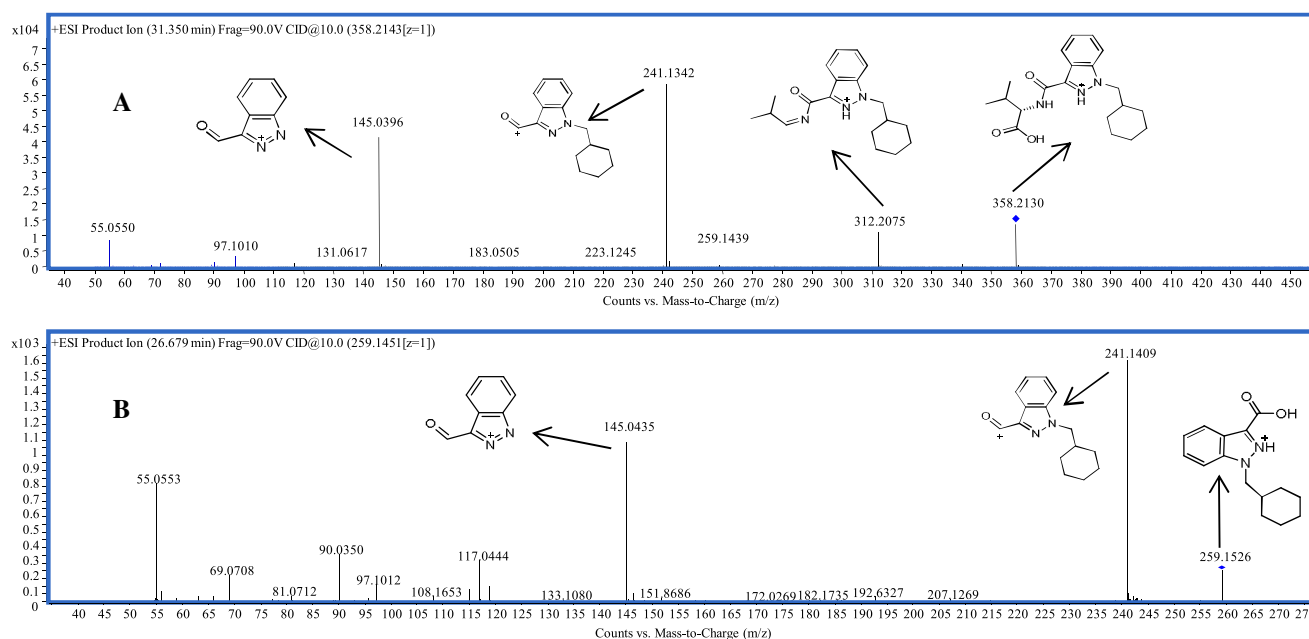


**Figure 4.** Fragmentation (MS/MS) spectrum of AB-CHMINACA carboxylated metabolites, M21 (A) and M20 (B).

the carboxylic moiety is slightly less polar than the amide moiety, the proposed structure of M21 is consistent with M21 retention time value being slightly higher than that of AB-CHMINACA (31.3 and 28.5 min, respectively; Table S1).

#### AB-CHMINACA metabolites produced by CYP enzymes

Fourteen hydroxylated metabolites were formed incubating AB-CHMINACA with HLMs and NADPH. Six mono-hydroxylated (M9 to M14) and six di-hydroxylated (M2 to M7) metabolites as well as two metabolites resulting from AB-CHMINACA *N*-dealkylation (M8) and from M8 hydroxylation (M1) were detected. None of these metabolites were detected in the negative control samples, and their retention times (mono-hydroxylated: between 17.0 and 24.3 min; di-hydroxylated: between 14.1 and 17.7 min; Table S1) confirm their higher polarity than AB-CHMINACA. For each of these metabolites, an increasing amount was formed with an increasing incubation time, protein concentration and substrate concentration (Figures 5, S1 and S2), confirming their metabolic nature. M9, M11 and M13 were likely the major mono-hydroxylated metabolites and M3 and M4 were the likely major di-hydroxylated metabolites detected (Figure S1). These results consistently suggest that these fourteen peaks are metabolites of AB-CHMINACA produced by CYPs only.

The structure of the fourteen hydroxylated metabolites was investigated using their MS/MS spectra. The fragmentation patterns of the M9-M13 mono-hydroxylated metabolites of AB-CHMINACA consistently contained the same 6 major product ions (Figure 6A; *m/z* error are reported in Table S1). The product ions at *m/z* 356.2012 and 328.2061 result from the loss of the distal amine and amide group, respectively. Also, the product ion at *m/z* 310.1941 results from the loss of water of *m/z* 328.2061. The product ions at *m/z* 257.1314 and 145.0404 are the indazole-3-carbaldehyde moiety with and without the hydroxylated methyl-cyclohexyl chain, respectively. The product ion at *m/z* 239.1206 resulted from a loss of water from *m/z* 257.1314. Altogether, the product ions in MS/MS spectra of M9-M13 consistently suggest that hydroxylation group occurs in the

methyl-cyclohexyl chain. In contrast, the fragmentation pattern of the mono-hydroxylated metabolite M14 suggests that the hydroxyl group is not bound to the methyl-cyclohexyl moiety. Compared to the fragmentation pattern of M9-M13, the product ions at *m/z* 257.1314, 239.1206, and 310.1941 (Figure 6A) were not present in M14 fragmentation spectra (Figure 6B) while a product ion at *m/z* 241.1326 was observed. This result strongly suggests that no hydroxylation of the methyl-cyclohexyl moiety occurred. The observed product ions at *m/z* 328.2011 and 356.1964 can be linked with a hydroxyl group bound to the isopropyl group (Figure 6B).

The fragmentation patterns of the six di-hydroxylated metabolites of AB-CHMINACA (M2 to M7) consistently contained the same 7 product ions (Figure 6C). Observed masses at *m/z* 372.1920 and 344.1968 are the result of the loss of the terminal amine and amide groups of the protonated parent ion (*m/z* 389.2176), respectively. The product ion at *m/z* 326.1869 results from the loss of a molecule of water from *m/z* 344.1968. The product ions at *m/z* 273.1245 and 145.0397 are the indazole-3-carbaldehyde moiety with and without the di-hydroxylated methyl-cyclohexyl group, respectively. The product ion at *m/z* 257.1291 and 239.1177 results from a loss of one or two molecules of water, respectively, from *m/z* 273.1245. The similarity of the fragmentation pattern of the di-hydroxylated metabolites of AB-CHMINACA with the fragmentation pattern observed for M9-M13 suggests that the two hydroxyl groups are bound to the methyl-cyclohexyl moiety.

Two extra metabolites of AB-CHMINACA were also identified. The first metabolite (M8) resulted from the loss of the terminal methyl-cyclohexyl chain (Figure 7A). The product ions *m/z* 244.1082 and 216.1134 result from the loss of the terminal amine and amide group, respectively, of the protonated precursor ion (*m/z* 261.1356). Also, the three major product ions can be explained by the lack of the methyl-cyclohexyl moiety, which suggest a *N*-dealkylation of AB-CHMINACA. M1 resulted from the hydroxylation of M8 (Figure 7B). The product ions at *m/z* 260.1059 and 232.1156 resulted from the loss of the terminal amine and amide groups, respectively. Both product ions at *m/z* 242.0948 and 214.0973 are formed through the loss of water from *m/z* 260.1059

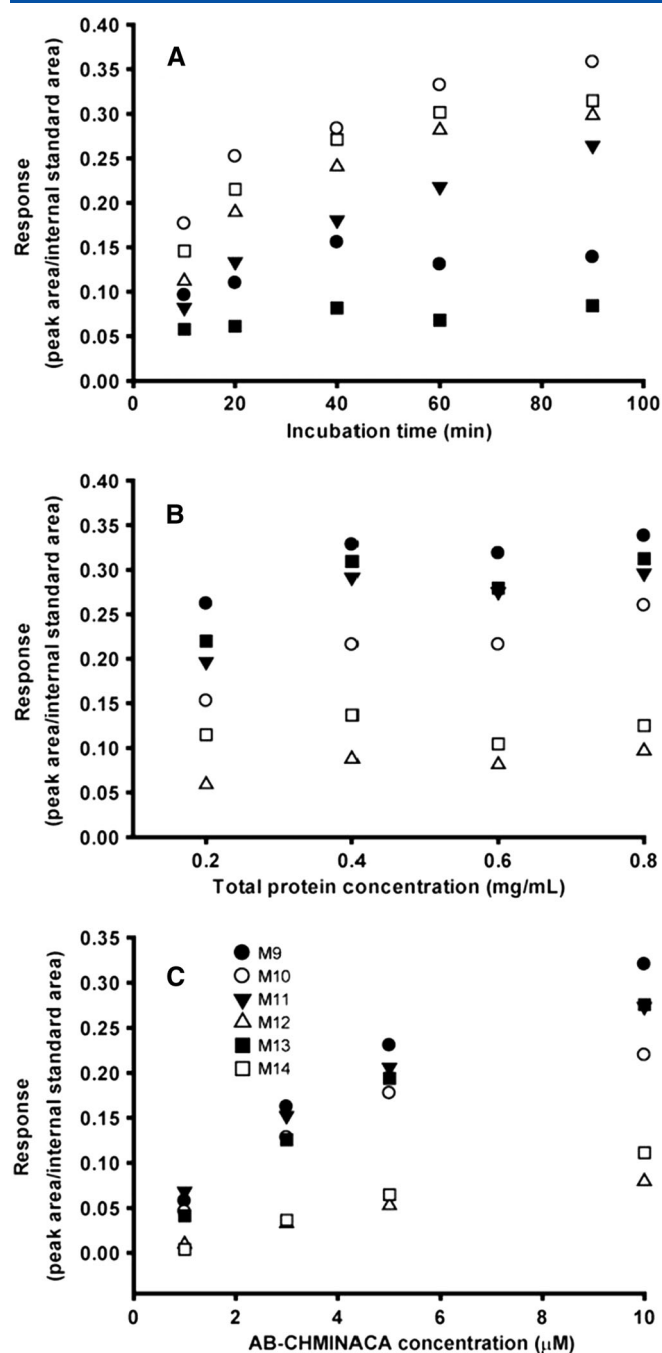


**Figure 5.** Amount of mono-hydroxylated (M9 to and M14) metabolites of AB-CHMINACA formed by CYPs as a function of (A) incubation time, (B) protein concentration and (C) AB-CHMINACA concentration.

and 232.1156, respectively. The absence of the cyclohexyl moiety in these structures together with the formation of a double bond, suggest that the hydroxyl group could only be bound to the isopropyl moiety. The product ions at  $m/z$  162.0668 and 145.0421 are the indazole-3-carbaldehyde moiety with and without the amide group, respectively.

#### AB-CHMINACA metabolites produced by amidase and CYP enzymes

Five mono-hydroxylated products of M21 (Table S1) were detected (M15 to M19). None of these metabolites (M15–M19) were observed

in the negative controls. The retention times of M15–M19 (between 19.5 and 23.7 min) suggest a higher polarity than that of AB-CHMINACA. Increasing incubation time, protein concentration or substrate concentration resulted in higher amounts of M15–M19 formed, with M15 being likely the major metabolite (Figure S3). These results consistently suggest that metabolites M15–M19 are mono-hydroxylated metabolites of AB-CHMINACA involving CYPs activity. Their chemical structures were further investigated using their MS/MS spectra. The fragmentation pattern of M15–M19 metabolites contained the same 4 major product ions (Table S1; Figure 7C). The product ion at  $m/z$  328.2039 results from the loss of the terminal carboxylic group of the protonated molecular ion ( $m/z$  374.2084). The product ions at  $m/z$  257.1285 and 145.0384 are the indazole 3-carbaldehyde with and without the hydroxylated methyl-cyclohexyl moiety. The product ion at  $m/z$  239.1180 results from a water loss from  $m/z$  257.1285. This fragmentation pattern consistently suggests that the hydroxyl group of M15–M19 is bound to the methyl-cyclohexyl moiety. M15–M19 can be formed through hydroxylation of M21 catalyzed by CYPs or through a hydrolysis of M9–M14 catalyzed by amidase.

#### AB-CHMINACA metabolites produced by UGT enzymes

No direct conjugation of AB-CHMINACA with glucuronic acid was observed. However, the positive control sample resulted in the formation of large amounts of 4-nitrophenol-glucuronide confirming the proper experimental design used (data not shown), which substantiate the negative results obtained for AB-CHMINACA direct conjugation.

Glucuronidation of AB-CHMINACA metabolites produced by CYPs and/or amidase was investigated and resulted in the formation of five metabolites: one glucuronidated metabolite of M20 (M24), two of M21 (M25 and M26), and two of M15–M19 (M22–M23; Table S2). None of these metabolites were detected in the negative control samples. The retention times of the glucuronidated metabolites were consistently lower than their putative substrates (M15–M21), which confirms the higher hydrophilicity of glucuronidated metabolites (Table S2). The structures of M22–M26 were further investigated using their MS/MS spectra patterns (Figure S4). A common fragmentation pathway for all the five glucuronidated metabolites was observed. The two major product ions of M25 and M26 were at  $m/z$  356.1951 and 175.0252, the former resulting from the loss of the glucuronic acid from the parent ion and the latter being the typical glucosyl fragment (Figure S4A). This observed fragmentation pattern suggests that the glucuronic acid was bound to the carboxylic moiety of M21. Similarly, M22 and M23 were fragmented into  $m/z$  175.0208 and 372.1836 (Figure S4B), which resulted from the same mechanisms explained for M25 and M26. The product ion at  $m/z$  328.2000 results from the loss of the carboxylic acid from  $m/z$  372.1836. As well, M24 was fragmented into  $m/z$  175.00191 and 257.1285 (Figure 4C), which resulted from the same mechanisms explained for M25 and M26 fragmentation pattern. The product ion at  $m/z$  213.1379 is the indazole with the methyl-cyclohexyl moiety, possibly resulting from the loss of the carboxylic group of  $m/z$  257.1285.

#### Positive control samples

Positive control samples for each family of enzymes of interest were prepared. Both tramadol metabolites were detected in large amounts in samples containing HLMs, tramadol and NADPH (mass error 2.96 and 9.59 ppm, respectively) and not in any negative

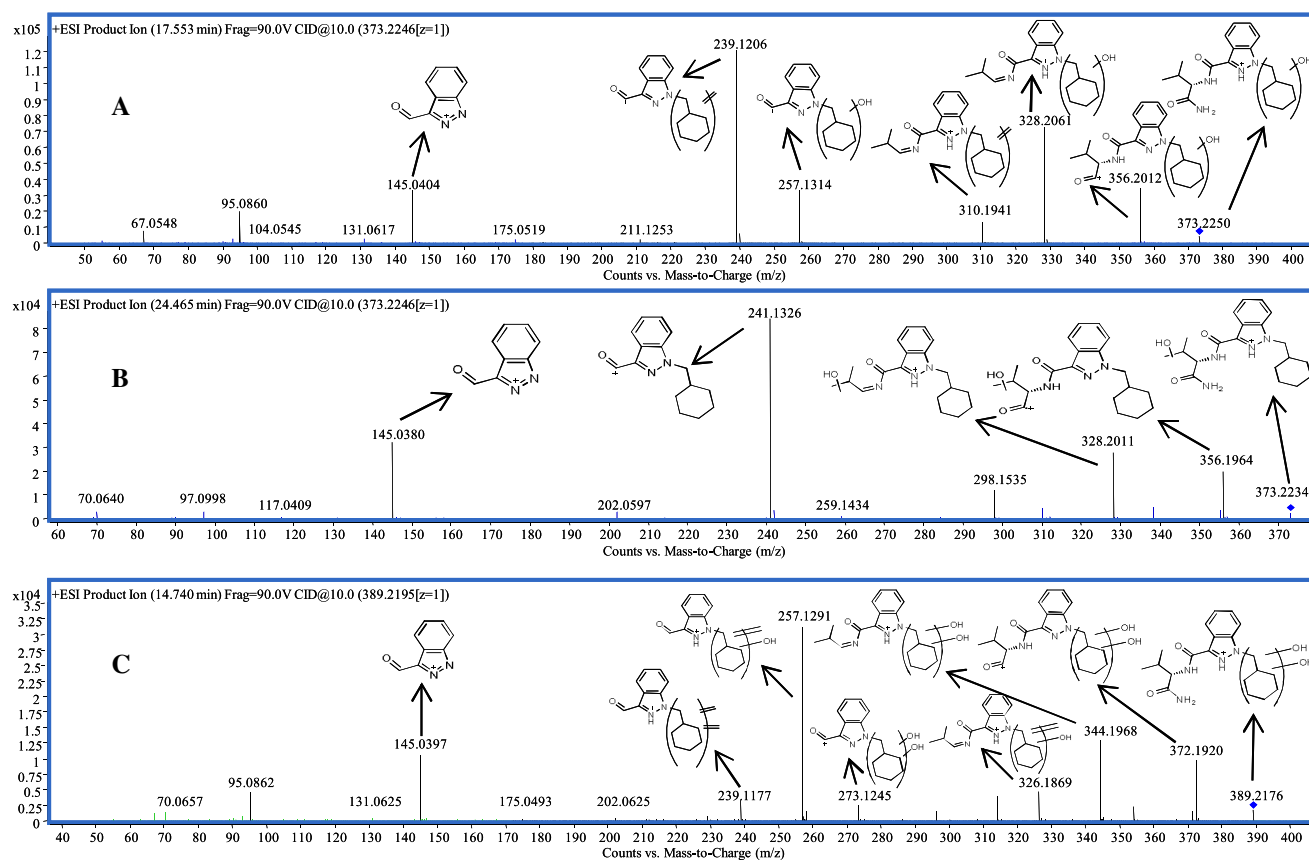


**Figure 6.** Fragmentation (MS/MS) spectra of mono-hydroxylated (M9–M13, A and M14, B) and di-hydroxylated (M2 to M7; C) metabolites of AB-CHMINACA formed by CYPs.

control sample (data not shown).<sup>[17]</sup> For amidase, benzoic acid, produced from benzamide, was detected in samples containing HLM and benzamide (mass error 4.11 ppm) and not in HLM and substrate negative controls (data not shown). For UGTs, 4-glucuronidated nitrophenol was detected in samples containing HLMs, 4-nitrophenol, alamethicin and UDPGA (mass error 5.41 ppm) and not in negative controls (data not shown). Collectively, these results confirm that the used HLMs contained catalytically active CYP, UGT, and amidase enzymes and that the experiments were properly conducted.

### Identification of the CYP enzymes involved in AB-CHMINACA *in vitro* metabolism

The individual human CYP enzymes involved in the metabolism of AB-CHMINACA were investigated using a panel of seven human rCYPs (Figure 8). Among all the metabolites of AB-CHMINACA formed in the presence of HLMs and NADPH, only (M1–M14) were also detected incubating AB-CHMINACA with the panel of human rCYPs. None of these metabolites were detected in human rCYP negative control sample. With the exception of M10, all the other metabolites detected were almost exclusively formed by rCYP3A4. Minor contributions to the formation of M9 (<20%), M11 (about 10%) and M14 (about 20%) were cumulatively given by rCYP1A2, 2B6, 2C9, 2C19 and 2D6. Formation of M10 was mainly catalyzed by rCYP3A4, 2C9 and 2C19 with a minor contribution of CYP2D6 (about 15%). Metabolites M15–M20 were not detected in the rCYP experiments, suggesting that their formation requires also enzyme (s) other than CYPs.

### Proposed *in vitro* metabolism pathway of AB-CHMINACA

The proposed *in vitro* metabolism of AB-CHMINACA is presented in Figure 9. From AB-CHMINACA six primary mono-hydroxylated (M9–M14) and two deaminated (M20 and M21) metabolites are produced by CYP and amidase enzymes, respectively. Also, CYP enzymes catalyze the formation of six di-hydroxylated metabolites (M2–M7) and the formation of another primary metabolite (M8), which is the result of *N*-dealkylation of AB-CHMINACA. M8 is then hydroxylated into M1 by CYPs, too. M21 is further metabolized by CYPs to produce 5 carboxylated/mono-hydroxylated metabolites (M15–M19), two of which are subsequently glucuronidated by UGTs (formation of M22 and M23). Finally, M20 and M21 are directly glucuronidated to form one (M24) and two (M25 and M26) metabolites.

### *In vivo* AB-CHMINACA metabolites

Several metabolites of AB-CHMINACA were detected in the urine sample obtained from a drug user (Figure S5). Two mono-hydroxylated (M9 and M11) and six di-hydroxylated (M2–M7) metabolites of ABCHMINACA as well as M8 were detected in the urine sample analyzed. Also, the carboxylated metabolites resulting from hydrolysis of the amide groups of AB-CHMINACA (M20 and M21) and two metabolites formed by M21 hydroxylation catalyzed by CYPs (M15 and M19) were present in the urine sample analyzed. Two glucuronidated metabolites, resulting from the glucuronidation of M21, were also detected (M25 and M26). Last, AB-CHMINACA was not detected in the urine sample analyzed.

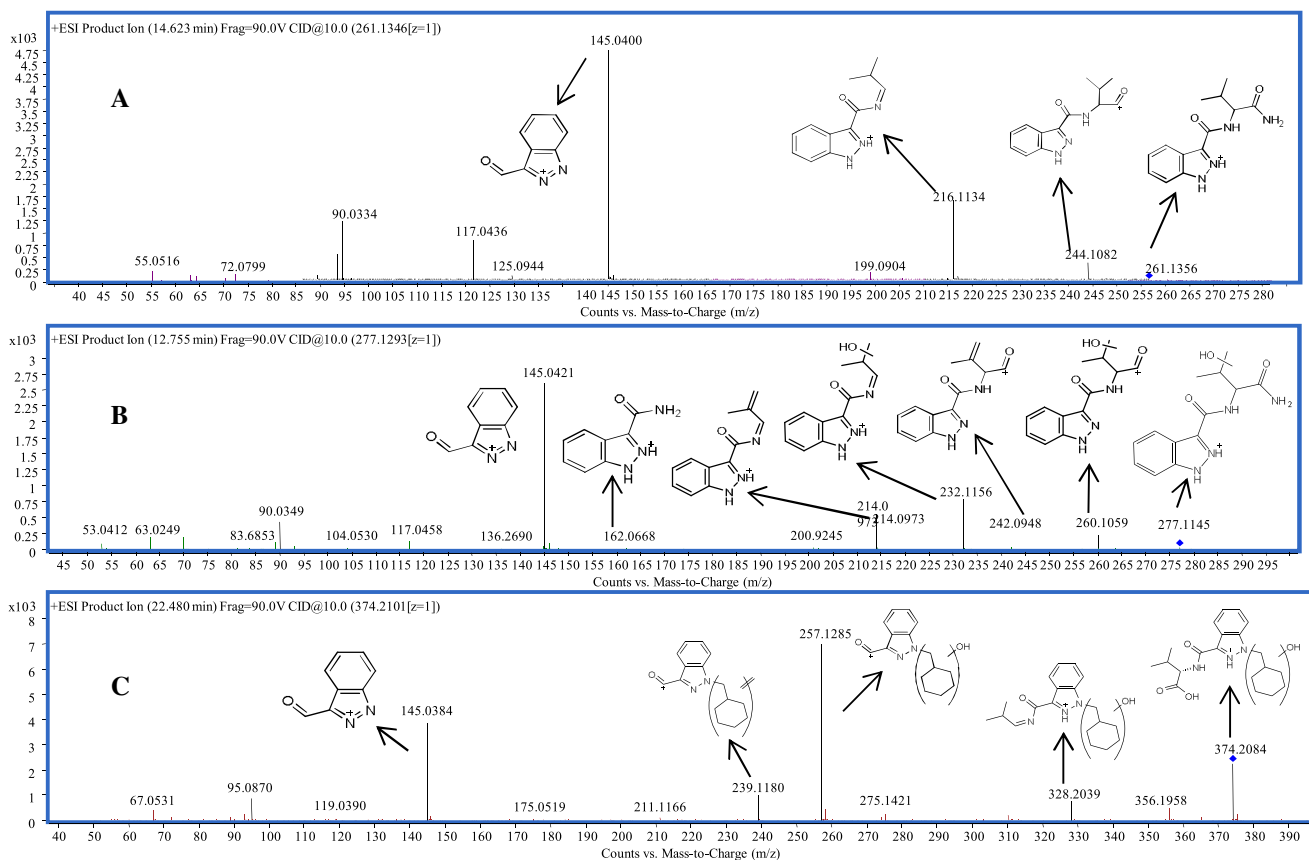


**Figure 7.** Fragmentation (MS/MS) spectra of minor metabolites of AB-CHMINACA formed by CYPs, M8 (A) and M1 (B) and of carboxylated and hydroxylated metabolites of AB-CHMINACA (M15–M19; C) formed by amidase and CYPs.

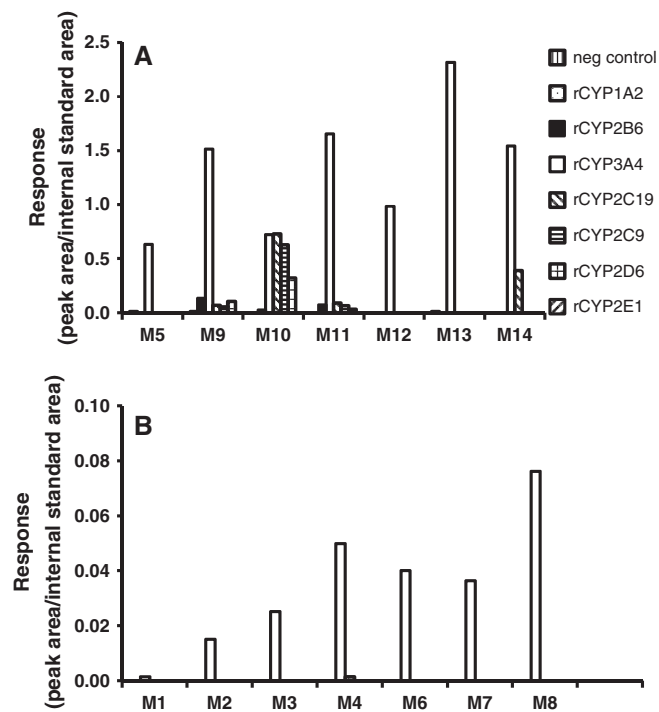


**Figure 8.** Human rCYPs involved in the formation of AB-CHMINACA metabolites.

## Discussion

This is the first study investigating the human *in vitro* and *in vivo* Phase I and Phase II metabolism of the synthetic cannabinoid AB-CHMINACA. The major *in vitro* metabolites were likely a carboxylic acid (M21) and six mono-hydroxylated metabolites (M9–M14). The hydrolysis of the two amide groups, likely catalyzed by amidase enzymes, resulted in the formation of M20 and M21. Since M21 was consistently formed in about ten folds larger amounts than M20, our data suggest that amidase enzymes preferentially hydrolyze the outer than the inner amide group of AB-CHMINACA. Five out of the six mono-hydroxylated metabolites of AB-CHMINACA detected (M9–M13) resulted from the hydroxylation of the methyl-cyclohexyl moiety and only M14 resulted from hydroxylation of the isopropyl group. M8, which was formed in lower amounts than M14, resulted from *N*-dealkylation of AB-CHMINACA. Therefore, the present results suggest that the main mechanism of AB-CHMINACA metabolism by CYP enzymes is a hydroxylation of the methyl-cyclohexyl moiety. The MS/MS spectra of all six di-hydroxylated metabolites (M2 to M7) and those of the five metabolites formed by hydroxylation of M21 (M15–M19) consistently provide further evidence that the main mechanism of AB-CHMINACA *in vitro* metabolism is the hydroxylation of the methyl-cyclohexyl moiety.

*In vitro* glucuronidation of primary and secondary metabolites of AB-CHMINACA occurred by the selective conjugation of the carboxylic acid moiety and not of any of the hydroxyl groups present in AB-CHMINACA Phase I metabolites. The specificity of the glucuronidation is supported by what follows: (1) the metabolites

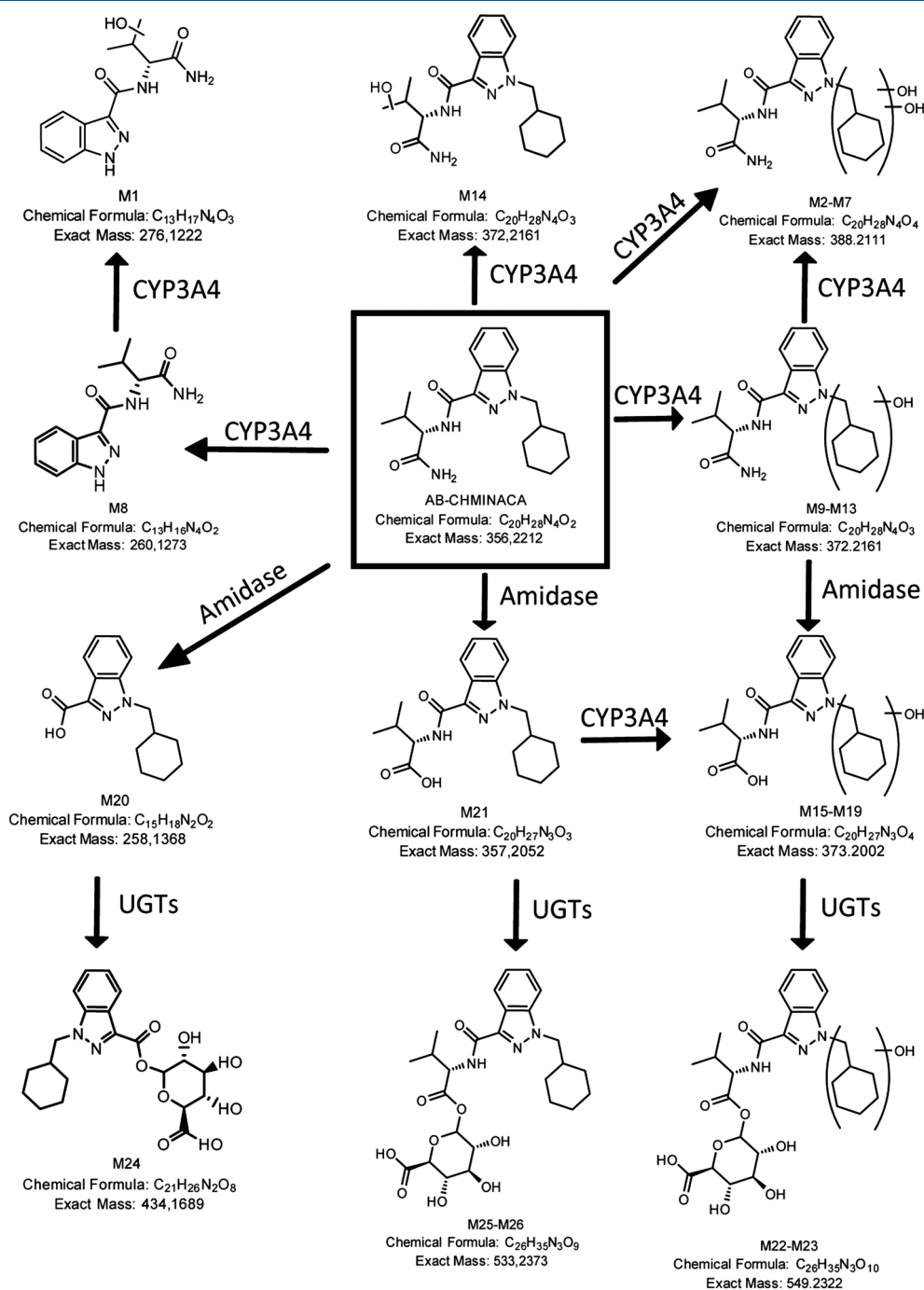


**Figure 9.** Proposed *in vitro* metabolism pathway of AB-CHMINACA.

containing a carboxylic acid moiety (M15–M21) were about half in number compared to those containing one or two hydroxylated groups and no carboxylic acid moiety (M1–M14); (2) M21 was formed in lower amounts than those of the major mono-hydroxylated metabolites (M9–M13), while M15–M20 were formed in lower amounts than those of the mono-hydroxylated (M9–M14) and di-hydroxylated (M2–M7) metabolites; and (3) although M15–M19 contained both a carboxylic and a hydroxyl group, only the carboxylic acid moiety was conjugated. Although glucuronidation can occur at hydroxyl and carboxylic groups,<sup>[18,19]</sup> some UGT enzymes have a marked preference for the carboxylic moiety rather than the hydroxyl group,<sup>[20]</sup> which is consistent with our

findings. The lack of standards for M15–M20 and the formation of glucuronidated metabolites of AB-CHMINACA only in small amounts prevented us to identify the contribution of individual UGT enzyme(s) in their formation using a panel of human recombinant UGTs or a combination of antibodies and chemical inhibitors specific for individual UGTs. Our data also shows that more than one glucuronidated metabolite can be formed from a substrate with only one site of expected glucuronidation (i.e., formation of M25 and M26 from M21). This result can be explained by the intramolecular rearrangement of 1-β-O-acyl glucuronide resulting from the migration of the acyl group to positions C-2, C-3 or C-4 of the carbohydrate moiety.<sup>[21]</sup> The rate of isomerization

is influenced by a number of parameters, including the structure of the aglycone,<sup>[21,22]</sup> which can also explain why only one glucuronidated metabolite was detected from M20.

Results obtained incubating AB-CHMINACA with a panel of seven human rCYPs show that rCYP3A4 has a key role in AB-CHMINACA metabolism. All hydroxylated metabolites of AB-CHMINACA formed by the rCYPs tested are almost exclusively formed by CYP3A4. The number, identity and relative amounts of metabolites formed by rCYP3A4 are in good agreement with those obtained in HLM incubations, therefore suggesting that the key role played by rCYP3A4 among the panel of human rCYPs used is representative of the CYP3A4 role in AB-CHMINACA metabolism *in vitro* (i.e., by HLM) and, possibly, *in vivo* in humans. The only partial inconsistency between the human rCYPs and the HLM incubations is the formation of M5 as major and minor dihydroxylated metabolite of AB-CHMINACA, respectively. We currently have not a valid explanation for this discrepancy. Although the metabolism of some synthetic cannabinoid drugs by HLMs has been investigated, to the authors' knowledge very limited attention has been paid to determine which CYP enzymes are involved in their *in vitro* metabolism.<sup>[14,15,23–28]</sup> Comparison of our data with those obtained about the JWH-018 *in vitro* metabolism by human rCYPs shows striking differences. While CYP3A4 was shown to have a key role in AB-CHMINACA *in vitro* metabolism, CYP1A2, 2C9, 2C19, and 2D6 (but not CYP2E1 and CYP3A4) were involved in the metabolism of JWH-018.<sup>[29]</sup> These results suggest that the human CYP enzymes involved in the metabolism of synthetic cannabinoids might differ substantially from one compound to the other.

The key role of CYP3A4 in *in vitro* metabolism of AB-CHMINACA suggests that (sub)chronic use of AB-CHMINACA could have multiple toxicological implications. CYP3A4 is the major CYP enzyme representing 30 to 60% of the total CYP content of human hepatic and intestinal microsomes,<sup>[30–32]</sup> is at least in part responsible for the metabolism of more than half of the currently marketed pharmaceuticals and is involved in the metabolism of several hormones.<sup>[33,34]</sup> Therefore, more research is necessary to evaluate whether (sub)chronic use of AB-CHMINACA could result in toxicological effects due to the alteration of the metabolism of therapeutic drugs and hormones.

Comparison of our AB-CHMINACA *in vitro* metabolism results with those of structurally related compounds like AB-PINACA, AB-FUBINACA, ADB-FUBINACA and AKB-48 reveals major overlaps and few differences in the metabolism mechanisms.<sup>[14,15,24]</sup> First, hydrolysis of the terminal amide group by amidase is a major metabolic pathway of AB-CHMINACA, AB-PINACA and AB-FUBINACA. Second, formation of several mono- and dihydroxylated metabolites of the non-aromatic terminal ring (AB-CHMINACA and AKB-48) or of terminal pentyl chain (AB-PINACA) is also a major mechanism. Third, with the exception of AB-FUBINACA, the indazole ring is not the part of the substrate that is preferentially metabolized. Fourth, CYP hydroxylation of the carboxylic acid metabolite likely produced by amidase generates intermediate or minor metabolites. Fifth, formation of glucuronidated conjugates of primary or secondary metabolites. However, differences in mechanisms of *in vitro* metabolism of AB-CHMINACA, AB-PINACA, AB-FUBINACA and AKB-48 can also be observed. A lack of hydrolysis of the inner and outer amide group in ADB-FUBINACA, of the inner amide group in AB-PINACA and AB-FUBINACA and of the only amide group in AKB-48 is in contrast with the formation of M20 from AB-CHMINACA.<sup>[14,15,24]</sup> Also, glucuronidation of only carboxylated moieties in AB-CHMINACA metabolism is in contrast with glucuronidation of hydroxyl groups

observed in AKB-48 metabolism and is probably due a structural difference with the adamantyl end-group.<sup>[24]</sup> These results suggest that *in vitro* metabolism of synthetic cannabinoids is mediated by the same families of enzymes (i.e., CYPs and UGTs) and produces similar types of metabolites (i.e., mono- and dihydroxylated metabolites), but small structural differences can have some influence on the observed metabolic pathway. The higher number of metabolites detected in our study and the importance of secondary and tertiary metabolites (including glucuronidated metabolites) for bio-monitoring drug use in humans strongly suggest that QTOF-based analysis is preferable over MS/MS-based analysis in screening the *in vitro* drug metabolism.

The majority of the *in vitro* AB-CHMINACA metabolites detected were also found in a urine sample collected from an AB-CHMINACA user. First, the same classes of AB-CHMINACA metabolites (i.e., mono- and dihydroxylated, carboxylated, carboxylated/hydroxylated and glucuronidated) detected *in vitro* were also detected in urine. Second, two out of the three major *in vitro* mono-hydroxylated metabolites of AB-CHMINACA (M9 and M11) were also detected in urine sample, together with M21, another major *in vitro* AB-CHMINACA metabolite. Third, all six dihydroxylated *in vitro* metabolites of AB-CHMINACA (intermediate metabolites) and M15 (the major metabolite among those resulting from the amidase- and CYP- mediated *in vitro* metabolism of AB-CHMINACA) were also detected in urine samples. Fourth, the two major *in vitro* glucuronidated metabolites of AB-CHMINACA (M25 and M26) were detected in human urine samples. Seen together these results suggest that (1) the experimental design and the data acquisition and processing strategy adopted in the present study provides results that are substantially predictive of the *in vivo* metabolism of the same drug in humans and (2) that characterization at least of secondary Phase I (i.e., dihydroxylated) metabolites and, preferentially, also of Phase II metabolites is very important when the *in vitro* metabolites are also used for drug screening purposes. It is also important to remark that target analysis of AB-CHMINACA only in the urine sample would have failed in determining the use of such drug. This result clearly stresses the key importance of *in vitro* drug metabolism screening experiments and the elucidation of the structures of the metabolites detected.

In conclusion, this is the first study to characterize the human *in vitro* and *in vivo* metabolism of AB-CHMINACA, a new synthetic cannabinoid. Major *in vitro* metabolites were four mono-hydroxylated metabolites and the carboxylated metabolite resulting from the hydrolysis of the outer amide group of AB-CHMINACA (M21). Six dihydroxylated metabolites, five mono-hydroxylated metabolites of M21 and five glucuronidated metabolites were also formed. Among the rCYPs tested, rCYP3A4 was the major CYP enzyme involved in the metabolism of AB-CHMINACA. The proposed *in vitro* metabolism pathway of AB-CHMINACA is consistent with that described analyzing a human urine sample, suggesting that the experimental approach used in the present study to characterize the *in vitro* metabolism of AB-CHMINACA is substantially predictive of its *in vivo* metabolism in humans.

### Acknowledgements

Noelia Negreira and Alexander L.N. van Nuijs acknowledge the University of Antwerp and FWO Flanders for their respective postdoctoral fellowships. This study has been partly financially supported by the EU through the FP7 (2007–2013) project under grant agreement #316665 (A-TEAM).

## References

- [1] United Nations Office on Drugs and Crime. The Challenge of New Psychoactive Substances, A Report from the Global SMART Programme. United Nations Office of Drugs and Crime, Vienna, Austria, **2013**.
- [2] European Monitoring Center for Drugs and Drug Addiction (EMCDDA). Perspectives on drugs: Synthetic cannabinoids in Europe. Available at [http://www.emcdda.europa.eu/attachements.cfm/att\\_212361\\_EN EMCDDA\\_POD\\_2013\\_Synthetic%20cannabinoids.pdf](http://www.emcdda.europa.eu/attachements.cfm/att_212361_EN EMCDDA_POD_2013_Synthetic%20cannabinoids.pdf) [3 February 2015].
- [3] B. K. Atwood, J. Huffman, A. Straiker, K. Mackie. JWH018, a common constituent of 'Spice' herbal blends, is a potent and efficacious cannabinoid CB receptor agonist. *Brit. J. Pharmacol.* **2010**, *160*, 585.
- [4] L. K. Brents, E. E. Reichard, S. M. Zimmerman, J. H. Moran, W. E. Fantegrossi, P. L. Prather. Phase I hydroxylated metabolites of the K2 synthetic cannabinoid JWH-018 retain *in vitro* and *in vivo* cannabinoid 1 receptor affinity and activity. *PLoS One.* **2011**, *6*, e21917.
- [5] S. J. Ward, E. Baizman, M. Bell, S. Childers, T. D'Ambr, M. Eissenstat, K. Estep, D. Haycock, A. Howlett, D. Luttinger. Aminoalkylindoles (AAls): A new route to the cannabinoid receptor? *NIDA Res. Monogr.* **1990**, *105*, 425.
- [6] G. A. Thakur, S. P. Nikas, A. Makriyannis. CB1 cannabinoid receptor ligands. *Mini Rev. Med. Chem.* **2005**, *5*, 631.
- [7] R. N. Kumar, W. A. Chambers, R. G. Pertwee. Pharmacological actions and therapeutic uses of cannabis and cannabinoids. *Anaesthesia.* **2001**, *56*, 1059.
- [8] S. Tai, W. E. Fantegrossi. Synthetic cannabinoids: Pharmacology, behavioral effects, and abuse potential. *Curr. Addict. Rep.* **2014**, *1*, 129.
- [9] R. Kikura-Hanajiri, N. Uchiyama, M. Kawamura, Y. Godo. Changes in the prevalence of new psychoactive substances before and after the introduction of the generic scheduling of synthetic cannabinoids in Japan. *Drug Test. Anal.* **2014**, *6*, 832.
- [10] N. Uchiyama, Y. Shimokawa, M. Kawamura, R. Kikura-Hanajiri, T. Hakamatsuka. Chemical analysis of a benzofuran derivative, 2-(2-ethylaminopropyl)benzofuran (2-EAPB), eight synthetic cannabinoids, five cathinone derivatives, and five other designer drugs newly detected in illegal products. *Forensic Toxicol.* **2014**, *32*, 266.
- [11] N. Uchiyama, S. Matsuda, D. Wakana, R. Kikura-Hanajiri, Y. Goda. New cannabimimetic indazole derivatives, N-(1-amino-3-methyl-1-oxobutan-2-yl)-1-pentyl-1H-indazole-3-carboxamide (AB-PINACA) and N-(1-amino-3-methyl-1-oxobutan-2-yl)-1-(4-fluorobenzyl)-1H-indazole-3-carboxamide (AB-FUBINACA) identified as designer drugs in illegal products. *Forensic Toxicol.* **2013**, *31*, 93.
- [12] K. Hasegawa, A. Wurita, K. Minakata, K. Gonmori, H. Nozawa, I. Yamagishi, K. Watanabe, O. Suzuki. Postmortem distribution of AB-CHMINACA, 5-fluoro-AMB, and diphenidine in body fluids and solid tissues in a fatal poisoning case: usefulness of adipose tissue for detection of the drugs in unchanged forms. *Forensic Toxicol.* **2015**, *33*, 45.
- [13] Drug Enforcement Administration. U.S. Department of Justice. Schedules of Controlled Substances: Temporary Placement of Three Synthetic Cannabinoids Into Schedule I. *Fed. Regist.* **2014**, *79*, 75767. Available at: [http://www.deadiversion.usdoj.gov/fed\\_regs/rules/2014/fr1219.htm](http://www.deadiversion.usdoj.gov/fed_regs/rules/2014/fr1219.htm) [3 February 2015].
- [14] R. Thomsen, L.M. Nielsen, N.B. Holm, H.B. Rasmussen, K. Linnet. The INDICES consortium. Synthetic cannabimimetic agents metabolized by carboxylesterases. *Drug Test. Anal.* DOI: 10.1002/dta.1731
- [15] T. Takayama, M. Suzuki, K. Todoroki, K. Inoue, J. Z. Min, R. Kikura-Hanajiri, Y. Goda, T. Toyo'oka. UPLC/ESI-MS/MS-based determination of metabolism of several new illicit drugs, ADB-FUBINACA, AB-FUBINACA, AB-PINACA, QUPIC, 5F-QUPIC and  $\alpha$ -PVT, by human liver microsomes. *Biomed. Chromatogr.* **2014**, *28*, 831.
- [16] Y. H. Zhao, J. Le, M. H. Abraham, A. Hersey, P. J. Eddershaw, C. N. Luscombe, D. Butina, G. Beck, B. Sherborne, I. Cooper, J. A. Platts. Evaluation of human intestinal absorption data and subsequent derivation of a quantitative structure-activity relationship (QSAR) with the abraham escriptors. *J. Pharm. Sci.* **2001**, *90*, 749.
- [17] V. Subrahmanyam, A. B. Renwick, D. G. Walters, P. J. Young, R. J. Price, A. P. Tonelli, B. G. Lake. Identification of cytochrome P-450 isoforms responsible for cis-tradamdol metabolism in human liver microsomes. *Drug Metab. Dispos.* **2001**, *29*, 1146.
- [18] R. H. Tukey, C. P. Strassburg. Human UDP-glucuronosyltransferases: Metabolism, expression and diseases. *Ann. Rev. Toxicol.* **2000**, *40*, 581.
- [19] U. A. Argikar. Unusual glucuronides. *Drug Metab. Dispos.* **2012**, *40*, 1239.
- [20] W. E. Gall, G. Zawada, B. Mojarrabi, T. R. Tephly, M. D. Green, B. L. Coffman, P. I. Mackenzie, A. Radomska-Pandya. Differential glucuronidation of bile acids, androgens and estrogens by human UGT1A3 and 2B7. *J. Ster. Mol. Biol.* **1999**, *70*, 101.
- [21] J. Hasegawa, P. C. Smith, L. Z. Benet. Apparent intramolecular acyl migration of zomepirac glucuronide. *Drug Metab. Dispos.* **1982**, *10*, 469.
- [22] R. W. Mortensen, U. G. Sidemann, J. Tjornelund, S. H. Hansen. Stereospecific pH-dependent degradation kinetics of R- and S-naproxen-beta-l-Oacyl- glucuronide. *Chirality.* **2002**, *14*, 305.
- [23] M. J. Jin, J. Lee, M. K. In, H. H. Yoo. Characterization of *in vitro* metabolites of CP 47, 497, a synthetic cannabinoid, in human liver microsomes by LC-MS/MS. *J. Forensic Sci.* **2013**, *58*, 195.
- [24] A. S. Gandhi, M. Zhu, S. Pang, A. Wohlfarth, K. B. Scheidweiler, H. F. Liu, M. A. Huestis. First characterization of AKB-48 metabolism, a novel synthetic cannabinoid, using human hepatocytes and high-resolution mass spectrometry. *AAPS J.* **2013**, *15*, 1091.
- [25] A. Wohlfarth, A. S. Gandhi, S. Pang, M. Zhu, K. B. Scheidweiler, M. A. Huestis. Metabolism of synthetic cannabinoids PB-22 and its 5-fluoro analog, 5 F-PB-22, by human hepatocyte incubation and high-resolution mass spectrometry. *Anal. Bioanal. Chem.* **2014**, *406*, 1763.
- [26] T. Sobolevsky, I. Prasolov, G. Rodchenkov. Detection of urinary metabolites of AM-2201 and UR-144, two novel synthetic cannabinoids. *Drug Test. Anal.* **2012**, *4*, 745.
- [27] A. Wintermeyer, I. Möller, M. Thevis, M. Jübner, J. Beike, M. A. Rothschild, K. Bender. *In vitro* phase I metabolism of the synthetic cannabimimetic JWH-018. *Anal. Bioanal. Chem.* **2010**, *398*, 2141.
- [28] A. Wohlfarth, S. Pang, M. Zhu, A. S. Gandhi, K. B. Scheidweiler, H. F. Liu, M. A. Huestis. First metabolic profile of XLR-11, a novel synthetic cannabinoid, obtained by using human hepatocytes and high-resolution mass spectrometry. *Clin. Chem.* **2013**, *59*, 1638.
- [29] K. C. Chimalakonda, K. A. Seely, S. M. Bratton, L. K. Brents, C. L. Moran, G. W. Endres, L. P. James, P. F. Hollenberg, P. L. Prather, A. Radomska-Pandya, J. H. Moran. Cytochrome P450-mediated oxidative metabolism of abused synthetic cannabinoids found in K2/spice: Identification of novel cannabinoid receptor ligands. *Drug Metab. Dispos.* **2012**, *40*, 2174.
- [30] T. Shimada, H. Yamazaki, M. Mimura, Y. Inui, F. P. Guengerich. Interindividual variations in human liver cytochrome P450 enzymes involved in the oxidation of drugs, carcinogens, and toxic chemicals: Studies with liver microsomes of 30 Japanese and 30 Caucasians. *J. Pharmacol. Exp. Ther.* **1994**, *270*, 414.
- [31] M. F. Paine, H. L. Hart, S. S. Ludington, R. L. Haining, A. E. Rettie, D. C. Zeldin. The human intestinal cytochrome P450 "pie". *Drug Metab. Dispos.* **2006**, *34*, 880.
- [32] S. A. Wrighton, W. R. Brian, M. A. Sari, M. Iwasaki, F. P. Guengerich, J. L. Raucy, D. T. Molowa, M. Vandenbranden. Studies on the expression and metabolic capabilities of human liver cytochrome P450III A5 (HLP3). *Mol. Pharmacol.* **1990**, *38*, 207.
- [33] F.P. Guengerich. in *Cytochrome P450: Structure, Mechanism and Biochemistry*. (Ed: P.R.O. de Montellano), Kluwer Academic and Plenum Publishers, New York, **2005**, pp. 377–463.
- [34] H. Yamazaki, T. Shimada. Progesterone and testosterone hydroxylation by cytochromes P450 2C19, 2C9, and 3A4 in human liver microsomes. *Arch. Biochem. Biophys.* **1997**, *346*, 161.

## Supporting information

Additional supporting information may be found in the online version of this article at the publisher's web site.